Theoretical Study of Dinitrogen Activation in Dinuclear V(II) and V(III) Hexacoordinated Complexes: *Ab Initio* Calculations on Various Model Compounds

Nazzareno Re, Marzio Rosi, and Antonio Sgamellotti*

Dipartimento di Chimica dell'Università, Perugia, Italy

Carlo Floriani

Section de Chimie, Université de Lausanne, Lausanne, Switzerland

Received June 3, 1994[⊗]

Ab initio RHF and CI calculations have been carried out on the $[H_3(NH_3)_2VN_2V(NH_3)_2H_3]$, $[H_3(NH_3)_2VN_2V(NH_3)_2H_3]^-$, and $[H_3(NH_3)_2VN_2V(NH_3)_2H_3]^{2-}$ complexes and related fragments in order to study the energetics and the mechanism of dinitrogen activation in dinuclear hexacoordinated complexes of vanadium(II) and vanadium(III). Various energy gradient optimizations have been performed on the complexes and the various fragments, followed by MRCI calculations on the stationary structures. The results indicate that in such complexes there is a near degeneracy between the states of high and low spin multiplicity and that dinitrogen is essentially from poorly to fairly activated depending on the oxidation state of the vanadium atoms and the spin multiplicity itself. The influence of vanadium coordination (tetrahedral versus octahedral) on dinitrogen activation has been discussed.

1. Introduction

There is a wide interest in dinitrogen coordination by metal complexes as it can be considered the first step in the nitrogen fixation process.[1−4] Several kinds of dinitrogen transition metal complexes have been observed, differing both in their nuclearity and in the bonding mode of the N_2 molecule.[5−7] Among them we will consider the terminal bridge bonding in dinuclear complexes, with a metal ion bound to each nitrogen atom in an end-on fashion. Activation of dinitrogen by bridging end-on coordination in dinuclear systems has been studied for a long time[8−13] and is particularly efficient for early transition metals.

Several *ab initio* investigations have been performed on mononuclear metal−nitrogen complexes[14−25] although only a few[26−31], mainly semiempirical[14,32,33] have been performed on dinuclear complexes.

In a mononuclear complex the binding of dinitrogen is usually qualitatively described by the Chatt−Dewar−Duncanson model[34] with σ donation from the nitrogen lone pair to an empty orbital of the metal atom and π back-donation from an occupied metal orbital to the empty nitrogen π^* orbital. In a dinuclear metal−dinitrogen complex the four-center M−N−N−M π interactions have been described through the qualitative molecular orbital scheme reported in Figure 1.[35] There are actually two sets of these four-center molecular orbitals which are obtained by linear combinations of respectively M d_{xy} and N p_x or M d_{yz} and N p_z

[⊗] Abstract published in *Advance ACS Abstracts,* May 15, 1995.

(1) Allen, A. D.; Harris, R. O.; Loescher, B. R.; Stevens, J. R.; Whiteley, R. N. *Chem. Rev.* **1973**, *73*, 13.
(2) Olivé, G. H.; Olivé, S. *Coordination and Catalysis*; Verlag Chemie: Weinheim, 1977.
(3) Chatt, J.; Dilworth, J. R.; Richards, R. L. *Chem. Rev.* **1978**, *78*, 859.
(4) da Camara Pina, C. L. M., Richards, R. L. Eds. *New Trends in the Chemistry of Nitrogen Fixation*; Academic Press: London, 1980.
(5) Henderson, R. A.; Leigh, G. J.; Picket, C. J. *Adv. Inorg. Chem. Radiochem.* **1983**, *27*, 197.
(6) Pez, G. P.; Apgar, P.; Crissey, R. K. *J. Am. Chem. Soc.* **1982**, *104*, 482.
(7) Jeffery, J.; Lappert, M. F.; Riley, P. I. *J. Organomet. Chem.* **1979**, *181*, 25.
(8) Sanner, R. D.; Manriquez, J. M.; Marsh, R. E.; Bercaw, J. E. *J. Am. Chem. Soc.* **1976**, *98*, 8351.
(9) Sanner, R. D.; Duggan, D. M.; McKenzie, T. C.; Marsh, R. E.; Bercaw, J. E. *J. Am. Chem. Soc.* **1976**, *98*, 8358.
(10) Schrock, R. R.; Wesolek, M.; Liu, A. H.; Wallace, K. C.; Dewan, J. C. *Inorg. Chem.* **1988**, *27*, 2050.
(11) Fryzuk, M. D.; Haddad, T. S.; Rettig, S. J. *J. Am. Chem. Soc.* **1990**, *112*, 8185.
(12) Duchateau, R.; Gambarotta, S.; Beydoun, N.; Bensimon, C. *J. Am. Chem. Soc.* **1991**, *113*, 8986.
(13) Beydoun, N.; Duchateau, R.; Gambarotta, S. *J. Chem. Soc., Chem. Commun.* **1992**, 244.
(14) Pelikan, P.; Boca, L. *Coord. Chem. Rev.* **1984**, *55*, 55.
(15) Lauher, J. H.; Hoffmann, R. *J. Am. Chem. Soc.* **1976**, *98*, 1729.
(16) Veillard, H. *Nouv. J. Chim.* **1978**, *2*, 215.
(17) Murrel, J. N.; Al-Derzi, A.; Leigh, G. L.; Guest, M. F. *J. Chem. Soc., Dalton Trans.* **1980**, 1425.
(18) Ondrechen, M. J.; Ratner, M. A.; Ellis, D. E. *J. Am. Chem. Soc.* **1981**, *103*, 1656.
(19) Hori, K.; Asai, Y.; Yamabe, T. *Inorg. Chem.* **1983**, *22*, 3218.
(20) Siegbahn, P. E. M.; Blomberg, M. R. A. *Chem. Phys.* **1984**, *87*, 189.
(21) Sakaki, S.; Morokuma, K.; Ohkubo, K. *J. Am. Chem. Soc.* **1985**, *107*, 2686.
(22) Sakaki, S.; Ohkubo, K. *J. Phys. Chem.* **1989**, *93*, 5655.
(23) Rosi, M.; Sgamellotti, A.; Tarantelli, F.; Floriani, C. *J. Organomet. Chem.* **1988**, *348*, C27.
(24) Rosi, M.; Sgamellotti, A.; Tarantelli, F.; Floriani, C.; Cederbaum, L. S. *J. Chem. Soc. Dalton Trans.* **1989**, 33.
(25) Ciullo, G.; Rosi, M.; Sgamellotti, A.; Floriani, C. *Chem. Phys. Lett.* **1991**, *185*, 522.
(26) Rappé, A. K. *Inorg. Chem.*, **1984**, *23*, 995; **1986**, *25*, 4686.
(27) Bauschlicher, C. W., jr.; Pettersson, L. G. M.; Siegbahn, P. E. M. *J. Chem. Phys.* **1987**, *87*, 2129.
(28) Siegbahn, P. E. M. *Chem. Phys.* **1991**, *95*, 364.
(29) Blomberg, M. R. A.; Siegbahn, P. E. M. *Chem. Phys. Lett.* **1991**, *179*, 524.
(30) Fryzuk, M. D.; Haddad, T. S.; Mylvaganam, M.; McConville, D. H.; Rettig, S. J. *J. Am. Chem. Soc.* **1993**, *115*, 2782.
(31) Blomberg, M. R. A.; Siegbahn, P. E. M. *J. Am. Chem. Soc.* **1993**, *115*, 6908.
(32) Powell, C. B.; Hall, M. B. *Inorg. Chem.* **1984**, *23*, 4619.
(33) Goldberg, K. I.; Hoffmann, D. F.; Hoffmann, R. *Inorg. Chem.* **1982**, *21*, 3863.
(34) Dewar, M. J. S. *Bull. Soc. Chim. Fr.* **1951**, *18c*, 71. Chatt, J.; Duncanson, J. A. *J. Chem. Soc.* **1953**, 2939.
(35) Chatt, J.; Fay, R. C.; Richards, R. L. *J. Chem. Soc. A* **1971**, 2399. Treitel, J. M.; Flood, M. T.; March, R. E.; Gray, H. B. *J. Am. Chem. Soc.* **1969**, *91*, 6512. Sellmann, D. *Angew. Chem.* **1974**, *13*, 639.

0020-1669/95/1334-3410$09.00/0

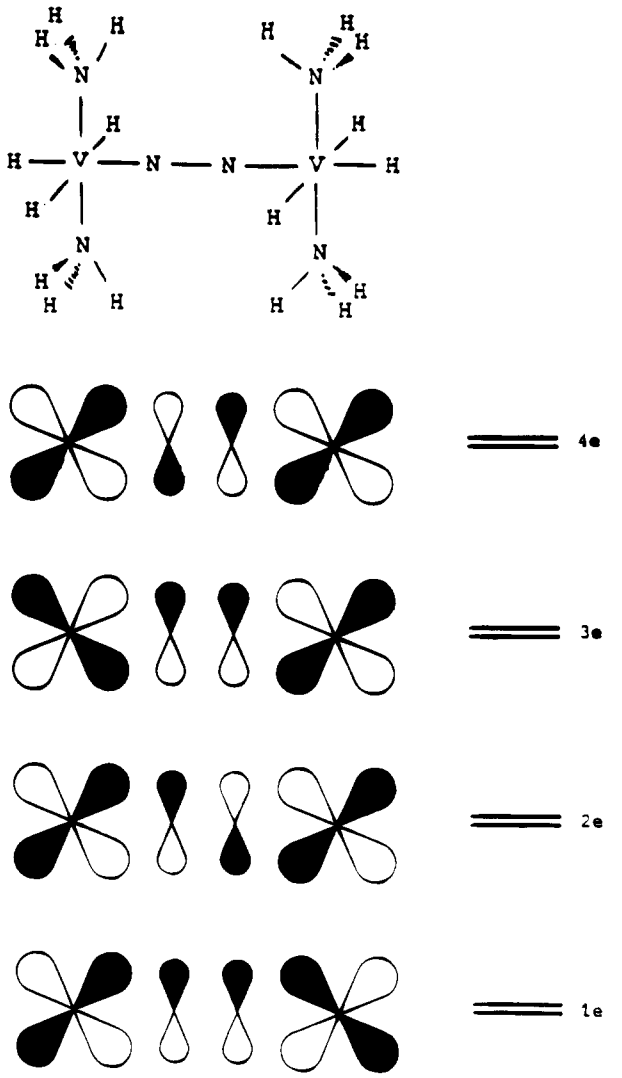

Figure 1. Schematic geometry of the $[H_3(NH_3)_2VN_2V(NH_3)_2H_3]^{0/-/-2}$ model complexes used in the calculations and representation of orbital interactions involved in the end-on bonded dinuclear N_2.

orbitals (with the y-axis determined by the σ bond direction). As overall result, we have four doubly degenerate energy levels whose energies increase with increasing nodal number of the molecular orbitals and which are designated as 1e, 2e, 3e, and 4e. The scheme is completed by the δ bond type orbitals built by the bonding and antibonding combinations of d_{xz} and $d_{x^2-z^2}$ orbitals which contribute practically nothing to the bonding because of the high M−M distance. The relative strength of the M−N and N−N bonds depends mainly on the occupancy number of these levels by the d electrons of the metals and the π electrons of N_2. Such strength considerations must take into account that occupation of the 2e levels (of π^* N_2 character) will result in a reduction of the N−N bond order, while occupation of the 3e levels (of π N_2 character) will increase the N−N bond order. We must moreover consider the mainly dinitrogen character of the 1e and 4e orbitals and metal character of the 2e and 3e orbitals. Most of the theoretical calculations performed on dinuclear N_2 complexes[26-31] have been interpreted in terms of the 1e−4e levels occupancy and also in terms of the relative metal−nitrogen composition of the corresponding orbitals.

It is commonly thought that dinitrogen activation is gauged by a lengthening in N−N bond distance with respect to free N_2 (1.10 Å). Indeed, the lengthening of the N−N bond distance is usually related to a reduction of the N−N bond order by direct comparison with the values for N−N double bond in azomethane (1.24 Å) and N−N single bond in hydrazine (1.47 Å). However, recent experimental studies on dinitrogen coordination in dinuclear systems[13,36] have shown that lengthening of the N−N distance is not always strictly related to its activation, very elongated N_2 molecules being sometimes inert to protonation.[37]

The present study has been inspired by the recent experimental reports on various dinitrogen dinuclear complexes of V(II) and V(III).[13,37,38] In particular, two distinct classes of complexes have been synthesized differing essentially for the coordination number on the vanadium centers: (i) complexes like $[Mes_3V-N_2-VMes_3(\mu\text{-Na})]^-[Na(diglyme)_2]^+$, **1**, and $[Mes_3V-N_2-VMes_3]^-[Na(diglyme)_2]^+$, **2**, [Mes = 2,4,6-$(CH_3)_3C_6H_2$; diglyme = $CH_3OCH_2CH_2OCH_2CH_2OCH_3$], respectively of V(II)−V(II) and V(II)−V(III) character, in which the two vanadiums are tetracoordinated; (ii) complexes like $\{[(o\text{-}Me_2NCH_2)C_6H_4]_2V(Py)\}_2(\mu\text{-}N_2)$, **3**, of V(II)−V(II) character, in which the two vanadiums are hexacoordinated. In spite of the similar geometrical parameters observed for the V−N−N−V unit, almost linear with V−N = 1.76−1.87 Å and N−N = 1.21−1.29 Å, these two classes sensibly differ both in electronic structure and in their chemical behavior. In particular, (i) the protonation of **1** and **2** leads to the evolution of NH_3 and N_2H_4 while the protonation of **3** leads to NH_3 and N_2; (ii) **1** and **2** show low or intermediate spin ground states (triplet and doublet, respectively) while complex **3** shows a high spin ground state (septet). Both these effects suggest that dinitrogen is more activated in complexes **1** and **2**, providing that the N_2 moiety is present in reduced form.

In a previous theoretical study[39] we investigated the complexes of the first class (with tetracoordinated vanadiums) pointing out the reasons for their peculiar electronic behavior and strong dinitrogen activation. In the present study we will theoretically investigate the complexes of the second class, with hexacoordinated vanadium. The only experimentally observed complex of this class is the $\{[(o\text{-}Me_2NCH_2)C_6H_4]_2V(Py)\}_2(\mu\text{-}N_2)$, of V(II)−V(II) character, see ref 13, which shows a fairly perturbed N_2 moiety with N−N = 1.23 Å and V−N = 1.83 Å.

However, more generally, we will study from a theoretical point of view the nitrogen activation in the dinuclear bridged end-on complexes of V(II) and V(III) octahedrically coordinated by amminic nitrogen and alkyl ligands (see Figure 1). We will consider as simplified models the $[H_3(NH_3)_2VN_2V(NH_3)_2H_3]$, **4**, $[H_3(NH_3)_2VN_2V(NH_3)_2H_3]^-$, **5**, and $[H_3(NH_3)_2VN_2V(NH_3)_2H_3]^{2-}$, **6**, species corresponding, respectively, to V(III)−V(III), V(II)−V(III), and V(II)−V(II) oxidation states. Actually, in order to reduce the size of our model complexes we had to introduce strong simplifications in real complex **3**—not only alkyl ligands were replaced by hydrogens and amide ones by ammonia, but also Py was replaced by H^-. This however should maintain all the general effects on dinitrogen activation due to change in vanadium coordination.

2. Computational Details

Basis Set. The s,p basis for vanadium was taken from the (12s6p4d) set of ref 40, with the addition of two basis functions to describe the 4p orbital[41] and the deletion of the outermost s function, while the V

(36) Leigh, G. J. *Acc. Chem. Res.* **1992**, *25*, 177.
(37) Buijink, J.-K. F.; Meetsma, A.; Teuben, J. H. *Organometallics* **1993**, *12*, 2004.
(38) Ferguson, R.; Solari, E.; Floriani, C.; Chiesi-Villa, A.; Rizzoli, C. *Angew. Chem. Int. Ed. Engl.* **1993**, *32*, 396 and unpublished results.
(39) Re, N.; Rosi, M.; Sgamellotti, A.; Floriani, C.; Solari, E. *Inorg. Chem.* **1994**, *33*, 4390.
(40) Ross, R.; Veillard, A.; Vinot, G. *Theor. Chim. Acta* **1971**, *20*, 1.
(41) Hood, D. M.; Pitzer, R. M.; Schaeffer, H. F., III. *J. Chem. Phys.* **1979**, *71*, 705.

Table 1. Total SCF and CI Energies (hartrees) for the $[H_3(NH_3)_2VN_2V(NH_3)_2H_3]^{2-}$ Complex in the Lowest Singlet, Triplet, Quintet, and Septet States and Its $V(NH_3)_2H_3^-$ and N_2 Fragments[a]

		SCF	CI
$[H_3(NH_3)_2VN_2V(NH_3)_2H_3]^{2-}$	$^1A_1$	−2221.9292	−2222.7106
$[H_3(NH_3)_2VN_2V(NH_3)_2H_3]^{2-}$	$^3A_1$	−2221.8860	−2222.6810
$[H_3(NH_3)_2VN_2V(NH_3)_2H_3]^{2-}$	$^5A_1$	−2222.1075	−2222.8544
$[H_3(NH_3)_2VN_2V(NH_3)_2H_3]^{2-}$	$^7B_1$	−2222.1329	−2222.8670
$V(NH_3)_2H_3^-$	$^4A_1$	−1056.6584	−1056.9285
N_2	$^1\Sigma_g$	−108.8481	−109.0937

[a] In the same geometry of the $[H_3(NH_3)_2VN_2V(NH_3)_2H_3]^{2-}$ $^7B_1$ complex.

Table 2. Main Geometrical Parameters (Bond Lengths, Å) for the Optimized Structures of $[H_3(NH_3)_2VN_2V(NH_3)_2H_3]^{2-}$ Complex in the Various Considered States

	N−N	V−N	V−H	V−NH_3
$^1A_1$	1.21	1.92	1.89	2.20
$^3A_1$	1.18	2.11	1.89	2.21
$^5A_1$	1.24	1.95	1.89	2.23
$^7B_1$	1.26	2.07	1.85	2.24

Table 3. Total SCF and CI Energies (hartrees) for the $[H_3(NH_3)_2VN_2V(NH_3)_2H_3]^-$ Complex in the Lowest Doublet and Quartet States and the $V(NH_3)_2H_3$ Fragment[a]

		SCF	CI
$[H_3(NH_3)_2VN_2V(NH_3)_2H_3]^-$	$^4A_2$	−2222.1625	−2222.9211
$[H_3(NH_3)_2VN_2V(NH_3)_2H_3]^-$	$^2A_2$	−2222.1435	−2222.8635
$V(NH_3)_2H_3$	$^3B_2$	−1056.6928	−1056.9837

[a] In the same geometry of the $[H_3(NH_3)_2VN_2V(NH_3)_2H_3]^-$ $^4A_2$ complex.

d basis was the reoptimized (5d) set of ref 42, contracted (4/1). This leads to an (11s8p5d) primitive basis for vanadium, contracted (8s6p2d). A double ζ expansion was used for all the other ligand atoms, with a (4s/2s) basis for hydrogen[43] and a (9s5p/4s2p) contraction for nitrogen.[43]

Methods. The calculations have been performed at two levels of accuracy. LCAO−SCF−MO scheme has been employed to derive ground state energies and wave functions for all the investigated structures of the systems and to perform the various geometry optimizations and transition state calculations. Multiple-reference configuration interaction (MRCI) calculations, including all the configurations with a CI expansion coefficient greater than 0.05, were subsequently performed on some of the stationary points determined at the SCF level. These calculations have been performed with the direct CI method.[44] To reduce the size of the CI problem, the V 1s, 2s, and 2p core orbitals have been frozen in all the calculations, while the highest virtual orbitals have been discarded. A multireference analogue[45] of Davidson's correction[46] was always added in the MRCI calculations to correct for the effect of unlinked clusters.

All computations were performed by using the GAMESS-UK program package,[47] implemented on IBM RS 6000 workstations.

Geometry and Geometry Optimization. In all the SCF calculations we have optimized essentially all the geometrical parameters with the only exception of the NH_3 and VN_2H_3 dihedral angles, fixed at 120° and 90°, respectively. The coordinate system has been chosen so that the *z* axis is the main symmetry axis. In the binuclear complexes this choice corresponds to the y axis parallel to the N-N direction. All the geometry optimizations have been performed using the quasi-Newton procedure available on the GAMESS-UK package.[47]

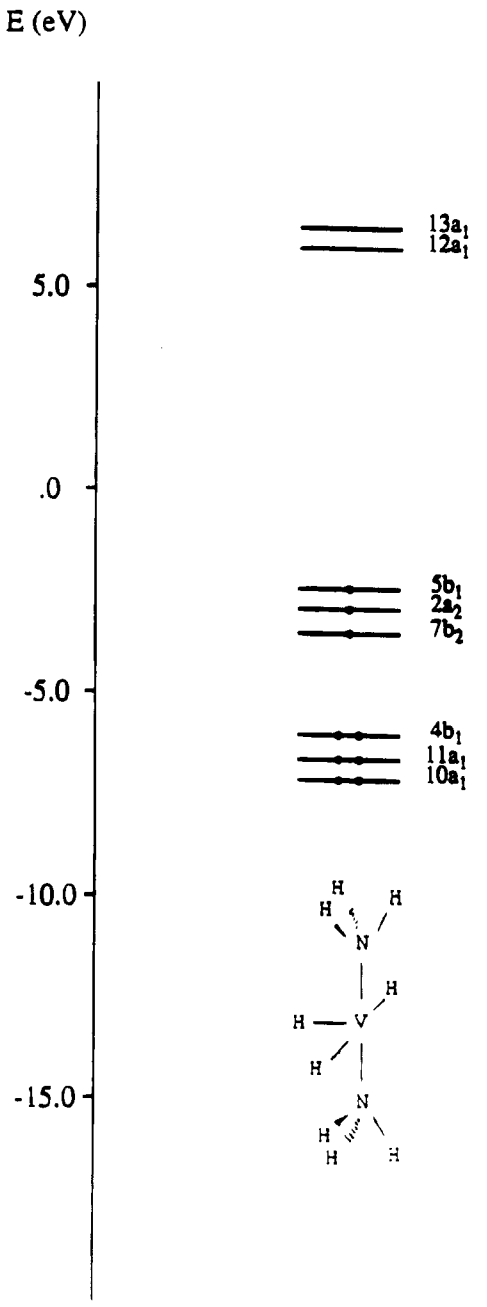

Figure 2. Molecular orbital diagram for the $V(NH_3)_2H_3^-$ fragment in the geometry of the optimized $[H_3(NH_3)_2VN_2V(NH_3)_2H_3]^{2-}$ complex.

3. Results and Discussion

Results. For the neutral $H_3(NH_3)_2VN_2V(NH_3)_2H_3$ species of V(III)−V(III) character, no stable state has been found with respect to fragmentation into N_2 and $[V(NH_3)_2H_3]$.

As a next step we have considered the dinuclear V(II)−V(II) nitrogen species performing SCF geometry optimization of the $[H_3(NH_3)_2VN_2V(NH_3)_2H_3]^{2-}$ complex in various spin states and evaluating the correlation energy through CI calculations on the optimized structures. We report the total energies in Table 1 and the main geometrical parameters of the optimized structures in Table 2. From Table 1 we see that the ground state, both at SCF and CI level, is a septet state of B_1 symmetry, with a quintet state of A_1 symmetry only 8 kcal mol^{-1} higher in energy, while the lowest triplet and singlet states are far higher in energy. However, if we take into account (i) the error due to the correlation energy, which is not completely corrected by a CI calculation based on the SCF wave function and favors the high-spin configuration, and (ii) the difference between the real complex **3**

(42) Rappé, A. K.; Smedley, T. A.; Goddard, W. A., III. *J. Chem. Phys.* **1981**, *85*, 2607.
(43) Dunning, T. H., jr. *J. Chem. Phys.* **1970**, *53*, 2823.
(44) Saunders, V. R.; Van Lenthe, J. H. *Mol. Phys.* **1983**, *48*, 923.
(45) Blomberg, M. R. A.; Siegbahn, P. E. M. *J. Chem. Phys.* **1983**, *78*, 5682.
(46) Davidson, E. R. In *The World of Quantum Chemistry*; Daudel, R., Pullman, B., Eds.; Reidel: Dordrecht, The Netherlands, 1974.
(47) Guest, M. F.; Sherwood, P. *GAMESS-UK User's Guide and Reference Manual*; Daresbury Technical Memorandum; Daresbury Laboratory: Daresbury, U.K., 1992.

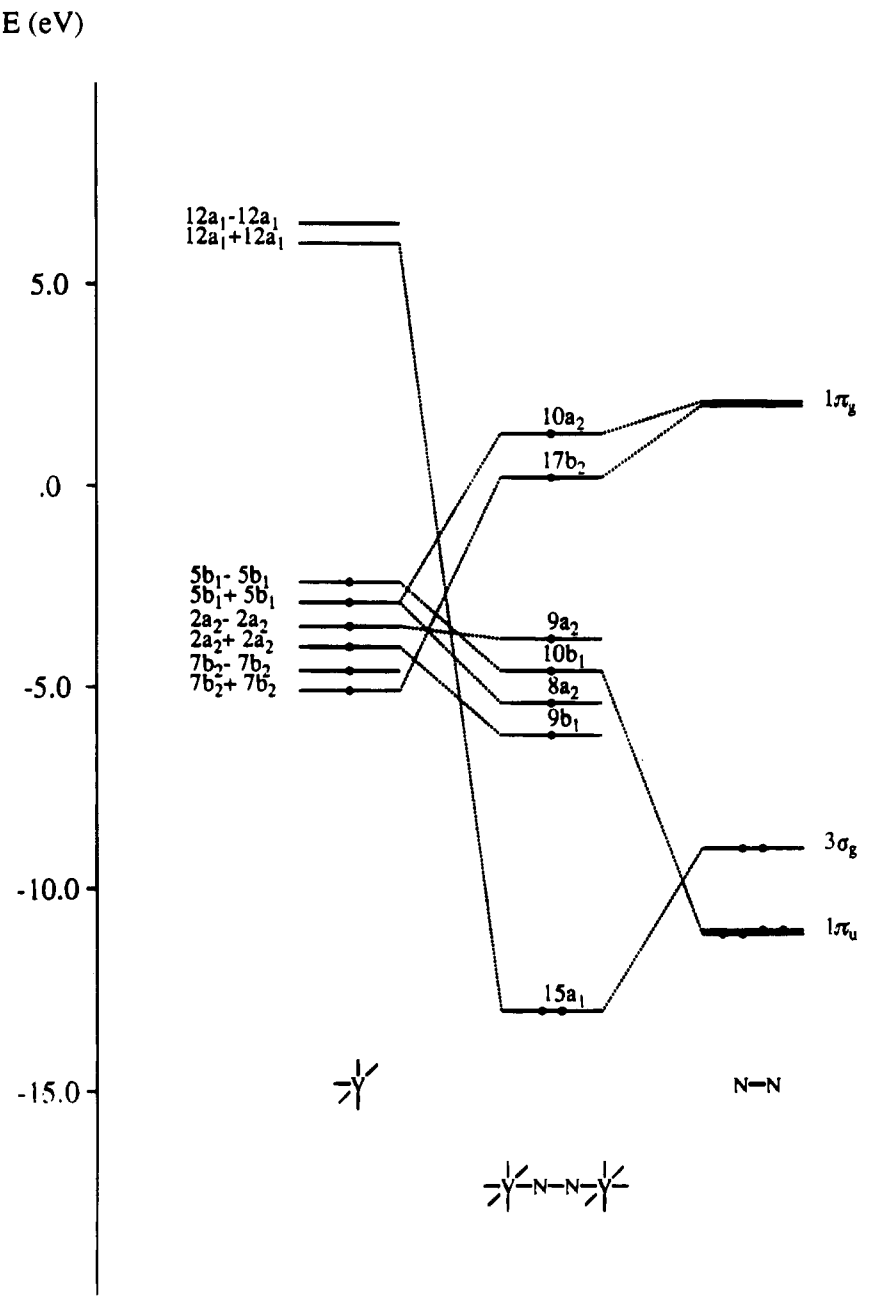

Figure 3. Molecular orbital diagram for the $[H_3(NH_3)_2VN_2V(NH_3)_2H_3]^{2-}$ complex in the $^7B_1$ state.

and our model, our calculations cannot provide a definitive assignment of the experimental ground state, the quintet and septet states having to be considered essentially degenerate.

This result is in agreement with the experimentally observed magnetic character of $\{[(o\text{-}Me_2NCH_2)C_6H_4]_2V(Py)\}_2(\mu\text{-}N_2)$, showing a value of magnetic moment of 3.47 μ_B per vanadium atom at 293 K which is close to that forecast for a quintet state (3.46 μ_B) and lower than that for the septet state (4.90 μ_B). With respect to our calculations, this observed value would suggest a quintet ground state although for a definitive answer experimental data of magnetic moment as function of temperature would be required. The observed high value of magnetic moment has been interpreted as arising from a small antiferromagnetic coupling between the two V(II) metallic fragments in quartet states, although this conclusion is not fully justified in absence of variable temperature magnetic moment data. This leads to a high spin $V^{II}(d^3)-V^{II}(d^3)$ picture for the electronic structure of the dinuclear species, which do not substantiate the point of view that $(\mu-N_2)$ has undergone a significant extent of reduction. This picture is however in contrast with the geometrical parameters of the complex (V−N = 1.83 Å and N−N = 1.23 Å) and its reactivity pattern (showing a partial reduction to ammonia for treatment with halogenidric acids) which implies a fairly activated dinitrogen moiety.

This apparent contrast can be explained from the detailed analysis of the bonding picture for our model complex in both the $^7B_1$ and $^5A_1$ states discussed below. We will see that there is essentially a two electron transfer from the vanadium centers to one or two molecular orbitals mainly localized on the N_2 moiety, so that the complex can be formally represented as $V(III)-N_2^{2-}-V(III)$.

The results of our calculations indicate a relevant perturbation of the dinitrogen molecule, due essentially to the population of the N_2 π^* orbitals.

We have then considered the monoanion $[H_3(NH_3)_2VN_2V(NH_3)_2H_3]^-$ of mixed valence V(II)−V(III) character, its SCF geometry optimization in the doublet and quartet states leads to the total energies reported in Table 3, while no sextet state has been found stable with respect to fragmentation into $[V(NH_3)_2H_3]^-$, $[V(NH_3)_2H_3]$, and N_2. In Table 3 we report also the CI energies obtained performing direct CI calculations on the two optimized structures. We see that at the more accurate CI level the quartet state lies much lower, 45 kcal mol^{-1}, than the doublet state.

The results of our calculation indicate a slight perturbation of the dinitrogen molecule.

Bonding Mode and Molecular Orbital Analysis. In order to point out the reasons of the apparent contrast between the magnetic and the

geometric properties of the model complex **6** and to localize the factors determining the difference between the two classes of tetracoordinated and hexacoordinated complexes, we performed an accurate analysis of the frontier molecular orbitals and therefore of the electronic structure of all the considered model molecules.

We begin to analyze the electronic structure of model complex **6** in the $^7B_1$ ground state which follows from an accurate analysis of the highest molecular orbitals and from the Mulliken population. A detailed and physically meaningful analysis of the highest molecular orbitals of $[H_3(NH_3)_2VN_2V(NH_3)_2H_3]^{2-}$ may be performed in terms of orbital interactions between preformed fragments which can be identified as one N_2 molecule and two $V(NH_3)_2H_3^-$ species. The $V(NH_3)_2H_3^-$ metallic fragment has been considered in the geometry that it presents in the SCF optimized structure of the whole complex, reported in Figure 2 together with its higher MO, which corresponds to a quasi-square base pyramidal geometry of C_{2v} symmetry. A sixth site is vacant in the metal fragment but occupied by the N_2 ligand in the full complex. The highest orbitals of $V(NH_3)_2H_3^-$ in the $^4A_1$ ground state are the $10a_1$, $11a_1$, and $4b_1$ which are involved in the σ V−H bonding, the three singly occupied $2a_2$, $5b_1$, and $7b_2$ which are almost pure d_{xy}, d_{xz}, and d_{yz} metal orbitals, respectively, and the two lowest unoccupied $12a_1$ and $13a_1$ corresponding to a combination of d_{z^2} and $d_{x^2-y^2}$ metal orbitals. In Figure 3 we show a diagram depicting the MO for the two $V(NH_3)_2H_3^-$ metallic fragments interacting with the MO of the bridging N_2 molecule to reproduce the energy levels of the upper valence region of the $[H_3(NH_3)_2VN_2V(NH_3)_2H_3]^{2-}$ complex. Actually in Figure 3 we report the energy levels for the two $V(NH_3)_2H_3^-$ fragments at the same distance observed in the whole complex (≃5 Å); due to extremely small interactions these levels consist of almost degenerate symmetric and antisymmetric combinations of those for the single fragment. In the same figure we report also the main valence orbitals of N_2 molecule, i.e. the bioccupied $3\sigma_g$, the doubly degenerate tetraoccupied $1\pi_u$ and the empty $1\pi_g$ MO.

This analysis reveals first of all that the main bonding orbital between vanadium and dinitrogen is the doubly occupied $15a_1$ which corresponds to the overlap between the N_2 $3\sigma_g$ orbital and an s, d vanadium hybrid orbital and describes a relevant σ donation from dinitrogen to vanadium. When we consider the six singly occupied orbitals, we see that four of them, $8a_2$, $9a_2$, $9b_1$, and $10b_1$, are of mainly metallic character and correspond to the symmetric and antisymmetric combinations of the vanadium d_{xy} and d_{xz} orbitals (the symmetric combination of d_{xy}, $8a_2$, being slightly mixed with one of the nitrogen π^* orbitals) while the remaining two, $10a_2$ and $17b_2$, are of mainly dinitrogen character only slightly mixed with the symmetric combinations of the vanadium d_{xy} and d_{yz} orbitals (describing a strong π back-donation from vanadium to dinitrogen).

Such a picture differs significantly from the usual Chatt−Dewar−Duncanson scheme, in which there is a strong overlap between the d orbitals of the metal atom and the dinitrogen π^* orbitals so that the back-donated electrons contribute also to a π V−N bond. Instead, we have essentially a two electron transfer from the vanadium centers to two singly occupied molecular orbitals mainly localized on the N_2 moiety, so that the complex can be formally represented as V(III)−N_2^{2-}−V(III). The above situation, although anomalous, is in principle more favorable to dinitrogen activation as it leads to the weakening of the N−N bond without the formation of a strong metal−nitrogen bond. However, in our complex we have only a single occupation of the two MO of mainly $\pi^*(N_2)$ character, so that the effects of such situation are not so strong.

In terms of the M−N−N−M molecular orbital scheme four of the singly occupied MO, the $17b_2$, $10a_2$, and $10b_1$ correspond to the 2e and 3e orbitals which are, respectively, of mainly unmixed dinitrogen and metallic character, while the remaining two, the $9a_2$ and $9b_1$, correspond to the 1δ orbitals of pure metal character. Although the population of one 3e ($d_\pi-\pi(N_2)$) orbital, $10b_1$, would generally suggest a low dinitrogen activation, the mainly N_2 character of the two 2e orbitals and metallic character of the 3e orbital observed in our case leads to an almost bielectronic population of the $\pi^*(N_2)$, as discussed above, and therefore to a relevant dinitrogen activation.

The above bonding picture is confirmed by a Mulliken population and spin population analysis of the septet wavefunction. In Table 4 we report the Mulliken gross atomic charge and spin population and the Mulliken population changes of the whole complex with respect to the $V(NH_3)_2H_3^-$, N_2 fragments. We see from it that the two N atoms gain about 1.2 electron charge unit, mainly localized on the $2p_x$ and $2p_z$ orbitals, i.e. on the two $1\pi_g$ antibonding orbitals of the N_2 molecule; at the same time there is a decrease of the population of the d_π orbitals (0.20 for the d_{xy} and 0.63 for the d_{yz}). Moreover the Mulliken spin population indicates 2.12 unpaired electron on the vanadium atoms, essentially localized on the d_{xy} and d_{xz} orbitals and 0.86 unpaired electrons on the nitrogen atoms, essentially localized on the p_x and p_z orbitals.

Table 4. Total Mulliken Atomic Charges and Spin Populations and Mulliken Population Changes of Various Orbitals for the $[H_3(NH_3)_2VN_2V(NH_3)_2H_3]^{2-}$ Complex in the $^7B_1$ State with Respect to the $V(NH_3)_2H_3^-$ and N_2 Fragments in the Same Geometry of the Corresponding Optimized Complex Structure

	atomic charge	spin pop.	pop. change
V	+1.06	2.12	−0.24
V s		0.02	+0.23
V p			+0.03
p_x			+0.02
p_y			+0.09
p_z			−0.08
V d		1.98	−0.50
$d_{x^2-z^2}$		0.03	+0.03
d_{y^2}		0.03	+0.30
d_{xy}		0.98	−0.20
d_{xz}		1.00	0.00
d_{yz}		0.06	−0.63
N	−0.61	0.86	+0.61
N s		0.01	−0.14
p_x		0.42	+0.47
p_y			−0.07
p_z		0.43	+0.35
H_e	−0.12		−0.12
H_a	−0.15		−0.15
NH_3	−0.53		−0.15

Table 5. Total Mulliken Atomic Charges and Spin Populations and Mulliken Population Changes of Various Orbitals for the $[H_3(NH_3)_2VN_2V(NH_3)_2H_3]^{2-}$ Complex in the $^5A_1$ State with Respect to the $V(NH_3)_2H_3^-$ and N_2 Fragments in the Same Geometry of the Optimized Complex Structure

	atomic charge	spin pop.	pop. change
V	+1.06	1.98	−0.23
V s		0.01	+0.22
V p			+0.02
p_x			+0.03
p_y			+0.08
p_z			−0.09
V d		1.97	−0.46
$d_{x^2-z^2}$		0.01	+0.02
d_{y^2}			+0.28
d_{xy}		0.01	−0.75
d_{xz}		0.96	−0.02
d_{yz}		0.98	+0.01
N	−0.47	0.01	+0.46
N s			−0.15
p_x			+0.41
p_y			−0.11
p_z			+0.31
H_e	−0.17		−0.11
H_a	−0.14		−0.13
NH_3	−0.55		−0.14

An analogous analysis of the $^5A_1$ shows a fairly different bonding picture which leads, however, to a similar situation for the dinitrogen activation. In fact, from the Mulliken orbital and spin population reported in Table 5 and from the diagram of the higher energy levels with the related interactions between the $V(NH_3)_2H_3^-$ and N_2 MO reported in Figure 4, it follows that in such a state the four singly occupied orbitals are almost pure metallic d orbitals while the highest bioccupied MO is mainly a dinitrogen π^* orbital slightly mixed with vanadium d_{xy} orbital. We still have, therefore, a dinitrogen formally reduced by two electrons (now paired on one of the two π^* orbitals) and two V(III) fragments.

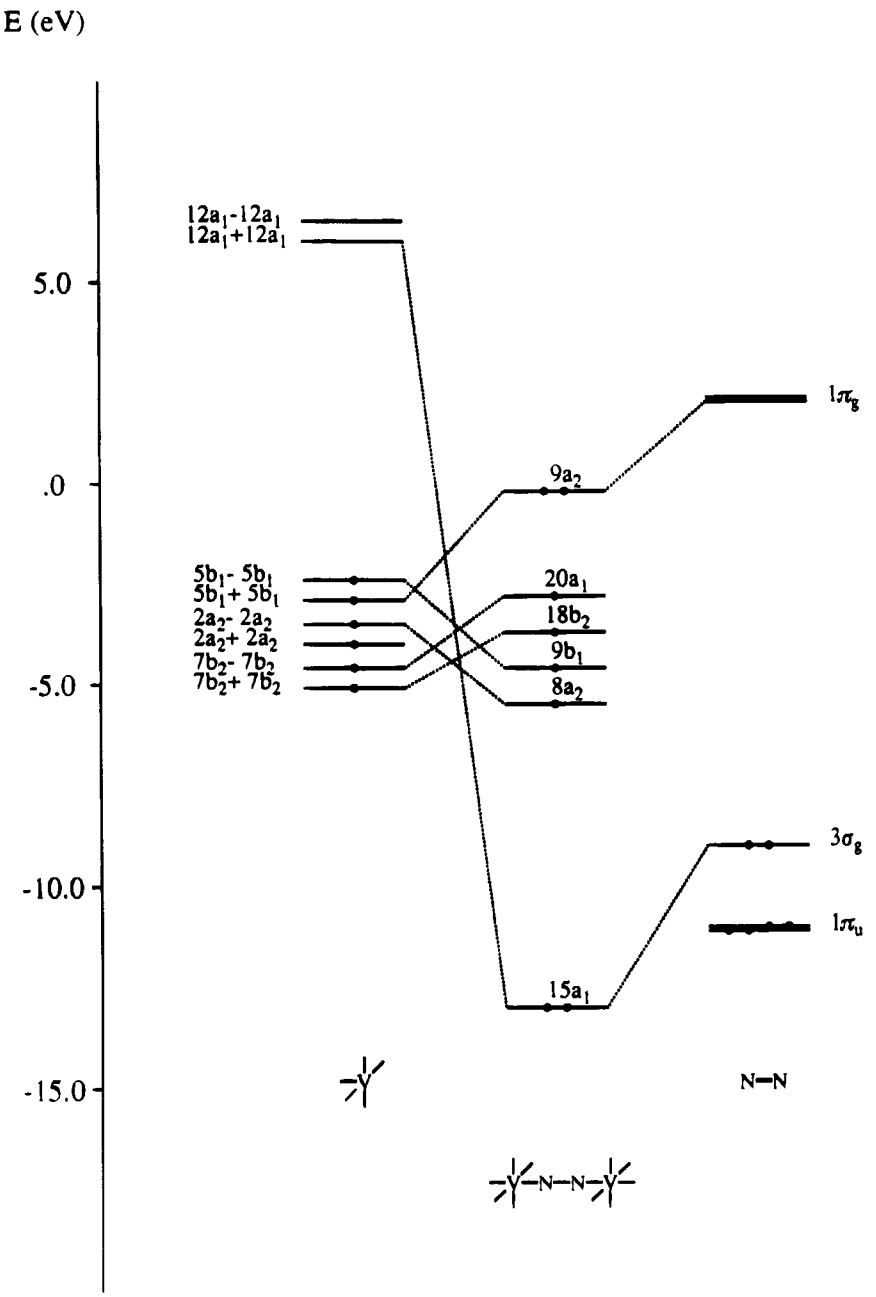

Figure 4. Molecular orbital diagram for the $[H_3(NH_3)_2VN_2V(NH_3)_2H_3]^{2-}$ complex in the $^5A_1$ state.

Altogether, the results of our calculations indicate a fairly high perturbation of the dinitrogen molecule, due essentially to the population of the N_2 π^* orbitals and a predominant role of σ donation with respect to π back-donation in the V−N bonding.

We will then analyze the bonding picture of complex **5** in the quartet ground state, in order to compare it with that observed for the dianion complex. First of all, we see that the relatively long V−N bond length (1.99 Å) and the short N−N one (1.14 Å), obtained by the SCF geometry optimization, indicate a poor dinitrogen perturbation. In Figure 5 we show a diagram depicting the MO for the two metallic fragments interacting with the MO of the bridging N_2 molecule to reproduce the energy levels of the upper valence region of the $[H_3(NH_3)_2VN_2V(NH_3)_2H_3]^-$ complex. Note that now we have two different metal fragments, $V(NH_3)_2H_3$ and $V(NH_3)_2H_3^-$. SCF calculations on the $V(NH_3)_2H_3$ species gave a $^3B_2$ ground state with a $d^1_{xy}d^1_{yz}$ configuration which, with respect to the $V(NH_3)_2H_3^-$ fragment, presents one less electron in the d_{xz} orbital. We have therefore chosen to report in Figure 5 as the "fragments" energy levels the energy levels for a hypothetical $[V(NH_3)_2H_3]_2^-$ dimer, obtained by averaging between the corresponding SCF monoelectronic levels for the two distinct fragments, taking the almost degenerate symmetric and antisymmetric combinations and putting only one electron on the symmetric combination of the d_{xz} levels.

From this diagram we see that the σ bond between vanadiums and dinitrogen is described by the doubly occupied $14a_1$ orbital (corresponding to the overlap between the $3\sigma_g$ orbital of N_2 and the 4s orbital of the two vanadiums). The highest doubly occupied $8a_2$ orbital corresponds to the overlap between the symmetric $3d_{xy}$ + $3d'_{xy}$ combination of vanadium orbitals and, only to a lesser extent, one of the two components of the virtual $1\pi_g$ orbital of N_2 and therefore describes π back-donation from vanadium to the dinitrogen. The dinitrogen is however slightly activated as the three singly occupied orbitals, the $20a_1$, $18b_2$, and $9b_1$, are all almost pure d orbitals of vanadium (the symmetric and antisymmetric combinations of d_{yz} and the antisymmetric combination of d_{xy} vanadium orbitals) and the doubly occupied MO describing π back-donation, $8a_2$, is of prevalent metallic character.

In terms of the M−N−N−M molecular orbital scheme, we note that the 2e orbitals correspond to the HOMO $8a_2$ orbital and the singly occupied $18b_2$ of essentially metal character, while the 3e orbitals correspond to the two singly occupied $20a_1$ and $9b_1$, of essentially metal character. In this scheme the unmixed character of at least one of the

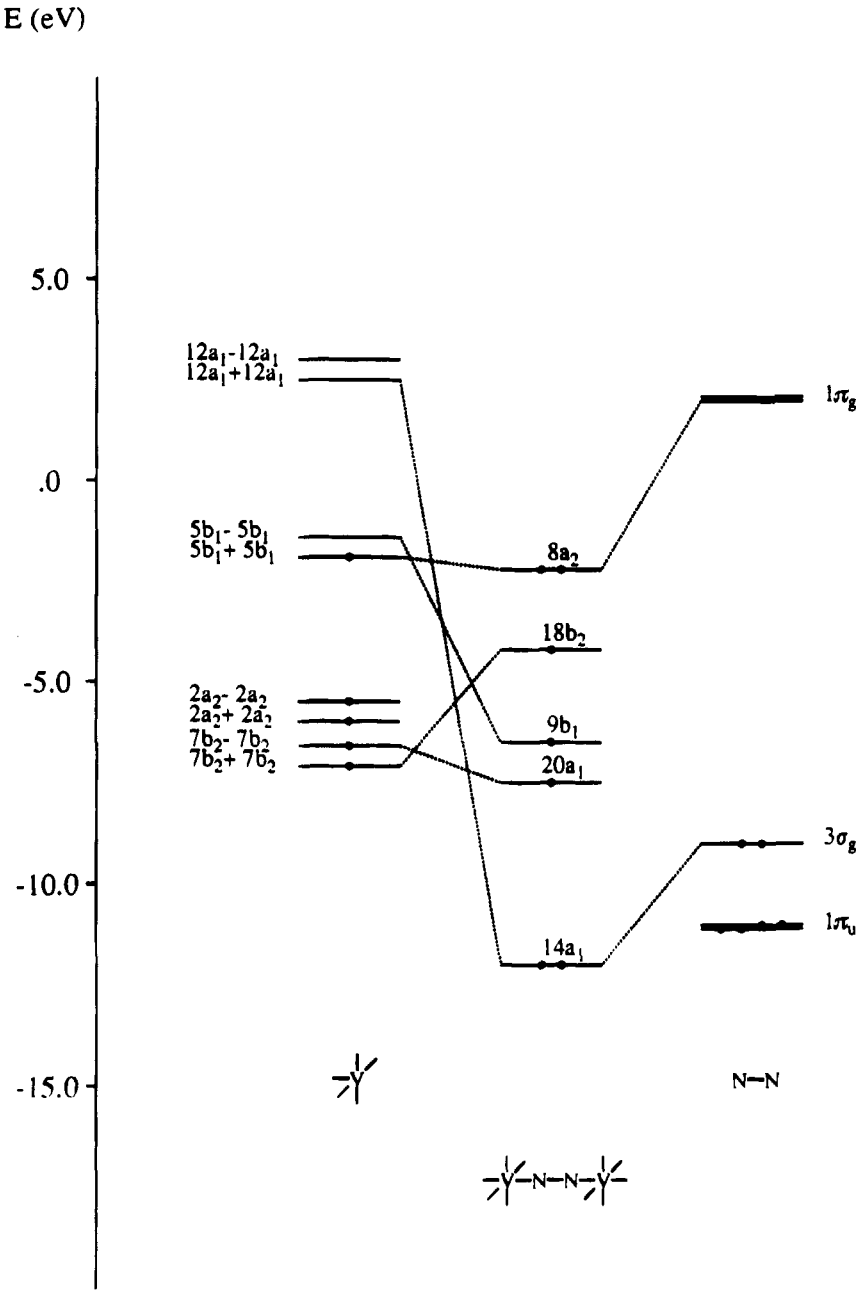

Figure 5. Molecular orbital diagram for the $[H_3(NH_3)_2VN_2V(NH_3)_2H_3]^-$ complex in the $^4A_2$ state.

two 2e orbitals and the occupation of the 3e orbitals determines the reduced activation of the dinitrogen as also shown by the values of the N−N and V−N bond distances.

Altogether, the results of the MO and Mulliken population analysis indicate a slight perturbation of the dinitrogen molecule, and suggest that σ donation plays again a predominant role with respect to π back-donation.

Thermodynamics. We have then considered the thermodynamics of the various complexes formation choosing the ground state for each considered complex and fragment, obtaining the following results at the most accurate CI level

$$2V(NH_3)_2H_3^- + N_2 \rightarrow [H_3(NH_3)_2VN_2V(NH_3)_2H_3]^{2-} \qquad \Delta E = +52 \text{ kcal mol}^{-1}$$

$$V(NH_3)_2H_3^- + V(NH_3)_2H_3 + N_2 \rightarrow [H_3(NH_3)_2VN_2V(NH_3)_2H_3]^- \qquad \Delta E = +53 \text{ kcal mol}^{-1}$$

The obtained values show that dinitrogen is endothermically bounded both in the dianion complex $[H_3(NH_3)_2VN_2V(NH_3)_2H_3]^{2-}$ and in the monoanion complex $[H_3(NH_3)_2VN_2V(NH_3)_2H_3]^-$. However, as we found a minimum for the electronic energy of both complexes, these are in principle stable due to an energy barrier toward dissociation into fragments.

Moreover, we must take into account that the theoretical calculations on the isolated species, while remaining very valuable in understanding the metal−N_2 interaction, the charge distribution, and the activation degree of N_2, are not very appropriate for justifying the energetics concerning the formation of the above N_2 complexes for a very important aspect: the driving force for the reaction should not be associated with the fragment assembly as reported in equations above but rather with the formation and solvation of the countercations.

Influence of the Coordination Number. It is interesting to discuss the influence of the vanadium coordination (pseudotetrahedral versus pseudooctahedral) on the dinitrogen activation in these dinuclear complexes. For this comparison we will consider only complexes of V(II)−V(II) character which are the only experimentally observed for both kinds of coordination, i.e. complex **6** for hexacoordination and complex $[H_3VN_2VH_3]^-$,[39] **7**, the model of **2**, for tetracoordination. In this context, the most striking result is the enormous effect of the

different vanadium coordination on the ordering of the different spin states of these complexes. Indeed, in **6** the high spin states, quintet and septet, are more than 5 eV lower than the low spin states, singlet and triplet, reported as the ground and first excited states of **7**.[39] On the other hand, in **7** the high spin states were found to be unstable with respect to dissociation into fragments and, for the geometry of the triplet ground state, they were more than 4 eV above the ground state itself. We will discuss this and other effects due to different vanadium coordination in terms of the influence on the orbital pictures for complexes **6** nd **7** due to differences in the valence orbitals of the metallic fragments $[V(NH_3)_2H_3]^-$ and $[VH_3]^-$, respectively.

A first general effect is related to the average energy of the monooccupied levels, of mainly d character, in the metallic fragments. In the pentacoordinated $[V(NH_3)_2H_3]^-$ fragment the three monoccupied orbitals lie close in energy at about −2.3 eV while in the tricoordinated $[VH_3]^-$ fragment they lie at about −4 eV. This difference leads to two consequences when considering the interaction between two fragments and one dinitrogen molecule: (1) in the hexacoordinated dinuclear complexes the d_{xy} and d_{yz} orbitals are closer to the dinitrogen π^* orbitals and interact stronger with them so that back donation to N_2 is more effective; (2) in the hexacoordinated dinuclear complexes the bonding and antibonding combinations of the fragments d_{xy} and d_{yz} orbitals with the dinitrogen π^* orbitals (corresponding to the 2e and 4e MO in the general scheme) are closer in energy so that states of high spin multiplicity are favored. While the first effect would make dinitrogen activation stronger in the hexacoordinated complexes, the second effect is much less clear as it may lead to simultaneous changes in orbitals composition and orbital population. There are, however, other specific effects due to the change in the nature of the monoccupied orbitals of the metallic fragment. In particular the following two effects are observed.

(1) In the pentacoordinated fragments the d_{z^2} orbital is a virtual one, being raised in energy by the interaction with the apical ligand, while in the tricoordinated fragment it is monoccupied. This difference leads to a much weaker interaction between the d_{z^2} orbital itself and the dinitrogen σ_g orbital and therefore to a weaker σ bond between vanadium and nitrogen. This latter effect approximately counterbalances the first of the two former ones so that the intermediate dinitrogen activation observed in the hexacoordinated complexes is due to the population of the π^* orbitals of N_2.

(2) In the pentacoordinated fragment the $d_{x^2-y^2}$ orbital is a virtual one. Indeed, the lobes of the two $d_{x^2-y^2}$ orbitals will be engaged in the formation of the metal to ligand σ bonds: in the dinuclear complex one of the two corresponding δ orbitals drops to lower energy and becomes a VLσ orbital, while the other rises in energy and becomes a VLσ^* orbital. This effect makes only one δ set (the d_{xy} one) available in the V−N−N−V π bonding scheme and, in the states of high spin multiplicity, forces the electrons from 2e orbitals to fill the 4e orbitals, giving a contribution both to dinitrogen activation and to electrostatic bond between the metallic fragments and the dinitrogen moiety. On the other hand in the tricoordinated fragment the $d_{x^2-y^2}$ orbital is monoccupied and the corresponding δ set of the dinuclear complex is available in the V−N−N−V π bonding scheme so that in the states of high spin multiplicity the electrons from 2e orbitals fill only δ orbitals giving no contribution to dinitrogen activation or to V−N bonding. Actually in our earlier calculations[39] the quintet and septet states of the tetracoordinated dinuclear complexes were found unstable with respect to dissociation to the constituting fragments.

Conclusions

This study at *ab initio* RHF and CI level has shown that dinitrogen is (i) fairly perturbed in the $[H_3(NH_3)_2VN_2V(NH_3)_2H_3]^{2-}$ complex of V(II)−V(II) character, essentially because of a two electron transfer leading to a formal V(III)−N_2^{2-}−V(III) species; (ii) slightly perturbed in the $[H_3(NH_3)_2VN_2V(NH_3)_2H_3]^-$ complex of V(II)−V(III) character; and (iii) neither bonded nor perturbed in the $[H_3(NH_3)_2VN_2V(NH_3)_2H_3]$ complex of V(III)−V(III) character. There is therefore a strong dependence of the dinitrogen activation in the considered dinuclear complexes on the oxidation states of the two vanadium centers with a decrease of the activation passing from V(II) to V(III), as seen for the analogous tetracoordinated complexes; see ref 39. The influence of vanadium coordination (tetrahedral versus octahedral) on dinitrogen activation has been discussed and the main result is that hexacoordination favors high spin states. Moreover the peculiar magnetic behaviour of these two classes of complexes depends on the quasi-degeneracy of the higher monoelectronic levels, corresponding to nonbonding d−d and slightly bonding d−π^* interactions, whose order depends critically on both the vanadium oxidation state and the vanadium coordination.

Acknowledgment. The present work has been carried out within the "Progetto finalizzato CNR Materiali Speciali per Tecnologie Avanzate" and the COST D3 Action "Theory and Modelling of Chemical Systems and Processes". This work was done while N.R. held a CNR fellowship. Support by the Fond Nationale Suisse de la Recherche Scientifique is gratefully acknowledged.

IC940641T